

# Real-time tracking of neuronal network structure using data assimilation

Franz Hamilton,<sup>1</sup> Tyrus Berry,<sup>2</sup> Nathalia Peixoto,<sup>1</sup> and Timothy Sauer<sup>2</sup>

<sup>1</sup>*Electrical and Computer Engineering, George Mason University, Fairfax, Virginia 22030, USA*

<sup>2</sup>*Mathematical Sciences, George Mason University, Fairfax, Virginia 22030, USA*

(Received 17 May 2013; revised manuscript received 18 September 2013; published 21 November 2013)

A nonlinear data assimilation technique is applied to determine and track effective connections between ensembles of cultured spinal cord neurons measured with multielectrode arrays. The method is statistical, depending only on confidence intervals, and requiring no form of arbitrary thresholding. In addition, the method updates connection strengths sequentially, enabling real-time tracking of nonstationary networks. The ensemble Kalman filter is used with a generic spiking neuron model to estimate connection strengths as well as other system parameters to deal with model mismatch. The method is validated on noisy synthetic data from Hodgkin-Huxley model neurons before being used to find network connections in the neural culture recordings.

DOI: [10.1103/PhysRevE.88.052715](https://doi.org/10.1103/PhysRevE.88.052715)

PACS number(s): 87.19.lj, 07.05.Mh

## I. INTRODUCTION

A dynamic of particular interest in neuronal networks is the connectivity structure. Connectivity changes as a function of network development and in response to applied electrical or pharmacological stimuli. Tracking these changes is essential for understanding the underlying dynamical evolution of the network, and serves as a valuable tool for experimental interventions.

A method for tracking connectivity should ideally meet several criteria. First, it should be statistical in nature. A strictly statistically based method will require only a predetermined confidence level, removing the need to provide an arbitrary decision threshold or decide how to make conclusions from a receiver operating characteristic (ROC) curve. Second, the method should be robust to error. We are typically interested in error caused by system noise, and error caused by a mismatch in dynamics between acquired data and the model used to represent the data. Third, the method should have sequential, or real-time, implementation capability. Real-time analysis of a network's structure is particularly important in experimental scenarios where feedback is critical for determining or controlling the direction of the experiment. This article describes a method for tracking connectivity in neuronal networks that meets these three criteria.

Methods for detecting network links from complex time series have been the focus of several recent studies. The analysis of interactions between nonlinear processes was pursued in [1,2], and ideas from compressed sensing were introduced in [3]. The concept of Granger causality [4] has been exploited by calculating partial directed coherence in [5].

Parallel to these developments are a wide range of connectivity methods for spike train measurements. Higher moment methods such as coherence, joint densities, and cumulant spectra were pursued in [6–8]. An information theory approach was proposed in [9]. Maximum likelihood methods for spike train neuronal interaction were investigated in [10–13]. These methods do not meet the first criteria of being statistically based.

The Cox method, introduced for neural networks in [14] and refined in [15], was the first statistical test for connectivity in networks analyzed by spike trains. The method was expanded in [16] to include a test for changes in connectivity. While the

Cox method satisfies the first two criteria of being statistical and robust to error, it fails to meet the third. Data requirements were found in [16] to be at least  $10^3$  spikes per node, and prior to the conclusion of processing, the method provides no estimate of the network connectivity structure. Furthermore, if new data are acquired then the entire data set must be re-processed before it can be included in the estimate, making use of the Cox method more suitable for offline analysis.

In the following we report on the use of a parameter-augmented version of the ensemble Kalman filter (EnKF) to estimate connection strengths of a network of cultured neurons sampled by a microelectrode array (MEA). The Kalman filter [17] is a natural choice for this problem, because in addition to estimating the connection parameters it will estimate their uncertainties, which will allow a statistical test for connectivity on acquired time series to be developed. We will show that the method exhibits a robustness to error much like the Cox method, but offers a significant advantage in terms of application for real-time analysis. We begin by demonstrating the results of a feasibility study of the method applied to synthetic data where there is significant model error, followed by application to the *in vitro* neural culture network.

## II. NONLINEAR DATA ASSIMILATION FOR LINK TRACKING

For assimilation purposes, we posit a general nonlinear system with an  $n$ -dimensional state vector  $x$  and  $m$ -dimensional observation vector  $y$  evolving according to

$$\begin{aligned} x_{k+1} &= f(x_k, t_k) + w_k, \\ y_k &= h(x_k, t_k) + v_k, \end{aligned} \quad (1)$$

where  $w_k$  and  $v_k$  are Gaussian noise terms with covariance matrices  $Q$  and  $R$  respectively. An ensemble Kalman filter (EnKF) approximates a nonlinear system using a finite weighted ensemble [18]. We initialize the filter with state vector  $x_0^+ = 0_{n \times 1}$  and covariance matrix  $P_0^+ = I_{n \times n}$ . At the  $k$ th step of the filter we assume we are given an estimate of the state  $x_{k-1}^+$  and a covariance matrix  $P_{k-1}^+$ . We use the singular value decomposition to find the unique symmetric positive definite square root  $S_{k-1}^+$  of the matrix  $P_{k-1}^+$ . Using the algorithm of scaled unscented transformation

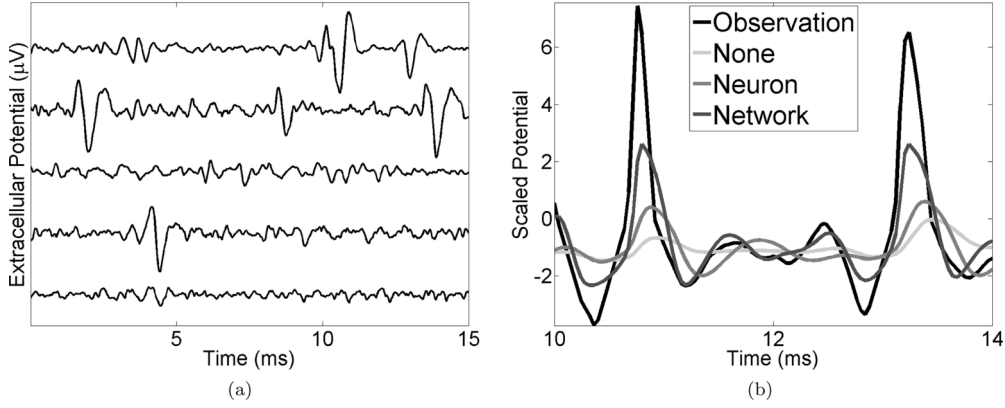


FIG. 1. (a) Small section of recorded extracellular potential *in vitro* (five traces shown). Sample neural spike wave forms from the MEA differ in shape from generic neuron models, which simulate intracellular currents. (b) Three assimilation results for top trace in (a). Observation (black) consists of preprocessed (see text) extracellular wave form compared with its intracellular model counterpart. When no parameters of the model are fit (marked None, light grey) the observation cannot track successfully. By fitting individual neuron parameters (marked Neuron, medium grey) more of the observation is tracked. When the full network parameters are fit in addition to the neuron parameters (marked Network, dark grey), the observation is fairly effectively tracked, showing the importance of including the network structure in assimilation.

(see for example [19]) a weighted ensemble of state vectors is generated. This ensemble is then propagated forward a single time step using the model  $f$  and observed with  $h$ . The mean of the resulting state ensemble is the *a priori* estimate  $x_k^-$  and the mean of the observed ensemble is the predicted observation  $y_k^-$ . Denoting the covariance matrices  $P_k^-$  and  $P_k^y$  of the resulting state and observed ensemble, and the cross-covariance matrix  $P_k^{xy}$  between the state and observed ensembles, the equations

$$\begin{aligned} K_k &= P_k^{xy} (P_k^y)^{-1}, \\ P_k^+ &= P_k^- - P_k^{xy} (P_k^y)^{-1} P_k^{yx}, \\ x_k^+ &= x_k^- + K_k (y_k - y_k^-) \end{aligned} \quad (2)$$

update the state and covariance estimates using the observation  $y_k$ .

For our purposes,  $f$  in (1) is chosen to be a generic spiking model. We used the Hindmarsh-Rose intracellular model [20] parametrized as in [21]:

$$\begin{aligned} \dot{V}_i &= a_i V_i^2 - V_i^3 - y_i - z_i + I_i + \sum_{j \neq i}^n \Gamma_{\text{HR}}(V_j) V_j + \sigma \dot{W}_{Vi}, \\ \dot{y}_i &= (a_i + \alpha_i) V_i^2 - y_i + \sigma \dot{W}_{yi}, \\ \dot{z}_i &= \mu_i (b_i V_i + c_i - z_i) + \sigma \dot{W}_{zi} \end{aligned} \quad (3)$$

for  $i = 1 \dots n$ , and where  $\Gamma_{\text{HR}}(V_j) = \beta_{ij} / (1 + 9e^{-10V_j})$  is a gating function that regulates the amount of input between neurons. Here  $V$  is the membrane variable,  $y$  (respectively,  $z$ ) represents the fast (respectively, slow) channel dynamics,  $I$  is the input current, and  $a, b, c, \alpha, \mu$  are model parameters whose values determine the different spiking behaviors of the neuron such as tonic spiking or bursting. The parameters  $\beta_{ij}$  represent the connectivity parameter from neural assembly  $j$  to neural assembly  $i$ , and  $W$  represents uncorrelated white noise of unit variance. The only observable used by the data assimilation procedure is the membrane voltage  $h(V, y, z) = V$ .

The choice of gating function  $\Gamma_{\text{HR}}(V_j)$  is used to force the model parameters to be fit from the spiking dynamics of the measured data, in addition to physiological plausibility. This

is based on a hypothesis that information is passed in a neural network primarily through spiking behavior, and we strive to avoid spurious fitting of model parameters from arbitrary resting potentials between spikes. We found through computer experiments with synthetic data that in the absence of a gating function the model parameters are easily fit from resting data, which overemphasizes the confidence in parameter fitting.

As discussed in [22–25], we can treat the  $l$ -dimensional parameter vector  $p$  as extra states of the model, with trivial dynamics. The augmented state vector, consisting of the original  $n$  model states and  $l$  parameters, is estimated by the EnKF. Figure 1(b) compares the reconstruction of the observable by the EnKF in three scenarios: with (1) fitting only the  $n$  state variables (no parameters), (2) the state variables plus model parameters  $\alpha_i, a_i$ , and  $I_i$ , and (3) the state, model and network parameters  $\beta_{ij}$ .

The extracellular wave form shown in Fig. 1 was recorded from a network of cultured mammalian spinal cord neurons plated onto a multielectrode array (MEA). An MEA simultaneously records the extracellular potential of spiking neurons plated near the array's electrodes. The neurons were extracted from embryonic day 18 (E18) mice, mechanically dissociated, and plated onto 64-channel MEAs at a density of about 200 000 cells per array. Cultures were kept under controlled temperature, 37°C, and humidity, 10% CO<sub>2</sub>, until recording at 28 days *in vitro*. Figure 1(a) shows several time traces of the recorded potential at separate electrodes.

Since the recorded extracellular potential wave form differs from the Hindmarsh-Rose wave form, preprocessing is required. We connected the recorded potential to its intracellular counterpart through the relationship  $dI/dt \approx E$  where  $E$  is the recorded extracellular potential and  $I$  is the intracellular potential [26]. The integration required was done using a simple moving average algorithm. The resulting approximation was then scaled as necessary to ensure stability when assimilated to our general model.

The design of the MEA allows for the possibility of multiple unit recordings at each electrode, although in the case reported

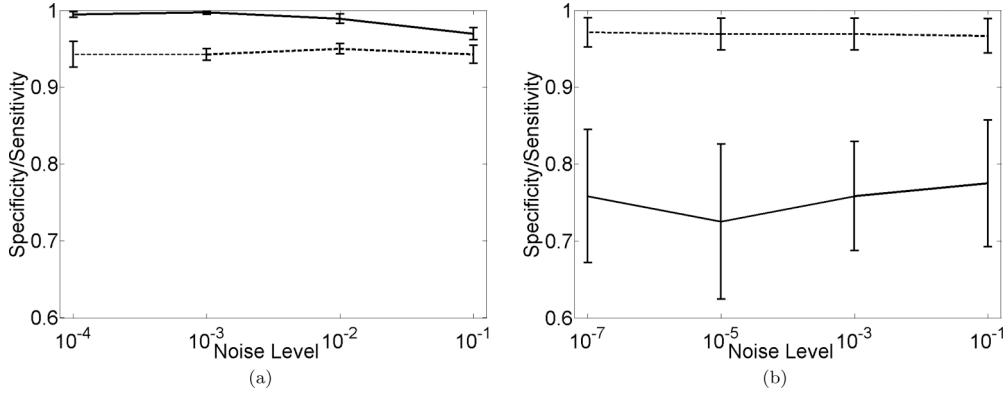


FIG. 2. Specificity (dotted line) and sensitivity (solid line) results of our method's identification of network links at the 95% confidence level when model error caused by noise is considered. Networks consist of (a) ten Hindmarsh-Rose neurons, (b) five Hodgkin-Huxley neurons with 40% network connectivity. In both cases, Hindmarsh-Rose was the EnKF network model. Error bars represent standard error over ten network realizations of length 8 sec. Identified links are those whose estimated  $\beta$  connectivity parameter is greater than two times their filter-estimated standard deviation.

here, offline analysis of the active electrodes showed single unit activity at each electrode. In a real-time analysis of network structure, sorting of individual units may not be feasible. Each electrode can thus be considered as a neural assembly, or population response, and subsequently be modeled as such. On the other hand, if analysis is to be done offline then units can be distinguished, for example, through principal component analysis (PCA) and use of a clustering algorithm.

The Hindmarsh-Rose equations were chosen for this problem since they can represent a significant range of neuronal behavior with only three dynamical variables. To resolve the possible error in estimated connectivity caused by unmodeled neuronal dynamics, some of the model parameters are left as free states to be estimated along with the model variables and connection parameters. These additional parameters give the EnKF extra degrees of freedom to resolve the model error and aid in the assimilation process. While there are more biophysically accurate models in the literature, the consequence of using these models is a more demanding estimation problem caused by the increase in variables and parameters. Our interest is in having a faithful representation of network connectivity, making this additional complexity unnecessary.

### III. STATISTICAL IDENTIFICATION OF NETWORK LINKS

The connectivity strength between neural assemblies will be represented by a parameter vector  $\beta$ , where  $\beta_{ij}$  indicates the connection parameter from neural assembly  $j$  to neural assembly  $i$ . Our goal is to use the recorded time series from each electrode to continuously estimate these  $\beta_{ij}$  parameters and determine which of the estimates are statistically significant, resulting in identified network links.

Using the ensemble Kalman filter produces an estimate of the error of the parameter estimate, given by the diagonal entry of the covariance matrix  $P_k^+$  corresponding to the parameter in question. Let  $\beta_{ij}$  be an estimated parameter in the state vector at time step  $k$  and let  $\sigma^2$  be the corresponding diagonal entry of the covariance matrix  $P_k^+$ . The standard confidence interval for  $\beta_{ij}$  with confidence level  $\gamma_0$  is  $[\beta - \kappa_{(1-\gamma_0)/2}\sigma, \beta + \kappa_{(1-\gamma_0)/2}\sigma]$

where  $\kappa_{(1-\gamma_0)/2}$  is the  $(1-\gamma_0)/2$  quantile of the normal distribution. Thus, we can apply a Wald test for connectivity parameter  $\beta_{ij} = 0$  by asking whether 0 lies in the above confidence interval.

Figure 2(a) shows that when data are fit with the correct model, the specificity and sensitivity results are correct at the 95% confidence level, independent of system noise. Here we used the Hindmarsh-Rose equations (3) both to generate data and as  $f$  in the EnKF equations.

To validate the method for use with real data, in Fig. 2(b) we test significant model error, caused by a mismatch in dynamics. Consider the Hodgkin-Huxley model [27] with original parameters as implemented by [28], expanded to a network of  $n$  equations,

$$\begin{aligned} \dot{V}_i &= -g_{Na}m^3h(V_i - E_{Na}) - g_Kn^4(V_i - E_K) \\ &\quad - g_L(V_i - E_L) + I + \sum_{j \neq i}^n \Gamma_{HH}(V_j)V_j, \\ \dot{m}_i &= a_m(V_i)(1 - m_i) - b_m(V_i)m_i, \\ \dot{h}_i &= a_h(V_i)(1 - h_i) - b_h(V_i)h_i, \\ \dot{n}_i &= a_n(V_i)(1 - n_i) - b_n(V_i)n_i \end{aligned}$$

with model functions

$$\begin{aligned} a_m(V) &= 0.1(V + 40)/1 - \exp[-(V + 40)/10], \\ b_m(V) &= 4 \exp[-(V + 65)/18], \\ a_h(V) &= 0.07 \exp[-(V + 65)/20], \\ b_h(V) &= 1/\{1 + \exp[-(V + 35)/10]\}, \\ a_n(V) &= 0.01(V + 55)/\{1 - \exp[-(V + 55)/10]\}, \\ b_n(V) &= 0.125 \exp[-(V + 65)/80] \end{aligned}$$

for  $i = 1, \dots, n$  and with gating function  $\Gamma_{HH}(V_j) = \beta_{ij}/(1 + e^{-10(V_j+40)})$  connecting neurons as in (3). The observables are the voltage variables  $V_i$  perturbed with noise, namely  $V_i + \sigma \tilde{W}_i$ . We assimilate these Hodgkin-Huxley data to the Hindmarsh-Rose model (3) and use the EnKF method to estimate the connectivity parameters.

The identification of network links using data from a significantly different neuron model presents a new challenge.

To handle the increased model error, we designate certain of the model parameters as free states while fixing others. We fix  $b = 9, c = 5, \mu = 0.001$  and leave  $a, \alpha, I$  as free states to be estimated along with the model variables. Additionally, we have to carefully tune parameters in the EnKF algorithm to prevent the covariance matrix from becoming degenerate and causing filter divergence, using a covariance inflation method. See [29] and the references therein for approaches to covariance inflation and tuning.

In an attempt to develop a fair test for our method, we simulate random networks of five noisy Hodgkin-Huxley neurons where each connected pair has a bidirectional relationship. That is, for every  $\beta_{ij}$  there is a  $\beta_{ji}$  in the network. Observational noise is used on the horizontal axis rather than system noise since the discrepancy in dynamics between the Hodgkin-Huxley data and our neuron model is already so large that the addition of extra system noise has no important effect.

Figure 2(b) shows that the EnKF method is successful in determining the neurons that are connected to one another, identifying that a statistically significant connection exists between a connected pair. As the amount of observational noise increases, our method maintains specificity around 95% showing that our results are statistically significant. Sensitivity persists around 70% showing that the method is finding the majority of the network links.

#### IV. LINK TRACKING

A significant application of this method is to detect the appearance and disappearance of connections in nonstationary networks, such as neural cultures. To verify the methodology for this purpose, we ran a simulated test of a Hodgkin-Huxley neural network where one of the network connections  $\beta_{ij}$  was turned on and off randomly. We used the above method to assimilate the voltage measurements only from the network, and purposely used the wrong model (Hindmarsh-Rose) in the EnKF, so that model mismatch was severe, and asked the method to track the changes.

We established the following protocol for determining the on/off transitions of the connection. When the connection is off, the protocol says to declare a transition from “off” to “on” when the mean estimated connection strength increases beyond the minimum (since the last “on” transition) of the confidence interval maximum; and vice versa for “off.” Figure 3 shows the ability of the method to detect these changes with minimal latency. The reconstructed parameter value of the  $\beta_{ij}$  as a function of time is plotted in the upper trace, along with 95% confidence limits. The lower grey trace is the imposed “on” time of the connection; in between these times the connection is set to zero. The lower black traces show the intervals at which the assimilation method finds a nonzero connection according to the above protocol. These results show the ability of the method to detect nonstationarities with minimal latency.

In Fig. 4, we apply the method to the *in vitro* data from the cell culture. Each panel of the figure shows the method’s continuous tracking of a different  $\beta_{ij}$  connectivity parameter with the appropriate 95% shaded confidence region over 160 sec of recorded data. A connection is detected with 95% confidence when the 95% confidence region does not include 0.

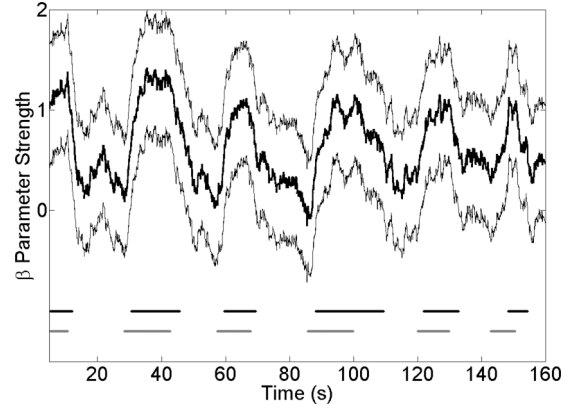


FIG. 3. Tracking results of a time-varying connection in a five-neuron network of Hodgkin-Huxley neurons over 160 sec of simulation data. Connection turned on/off randomly. Bottom traces of figure show the actual “on” time (grey bar) and the filter-estimated “on” time of the connection (black bar). Top traces of figure show the filter estimated connection strength and corresponding 95% confidence region.

Panels (a)–(c) show three estimated  $\beta_{ij}$  parameters and their respective confidence regions from a small network with five active electrodes. Panels (a) and (b) show identified links within the confidence level, while panel (c) shows a clear nonconnection. Panel (d) shows a  $\beta_{ij}$  parameter from a larger network with 12 active electrodes. Here is a difficult case. As the filter gains more information about the network, it is stating

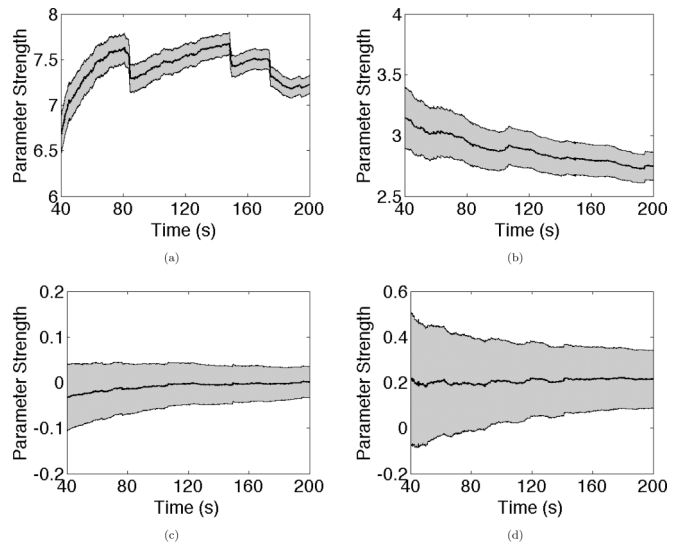


FIG. 4. Four example *in vitro*  $\beta_{ij}$  parameters tracked over 160 sec of data. Solid black line indicates the estimated connection strength and shaded grey area denotes 95% confidence region. A link is detected with 95% confidence when the 95% confidence region does not include 0. Panels (a)–(c) show three estimated  $\beta_{ij}$  parameters from a small network with five active electrodes, (a)  $\beta_{41}$ , (b)  $\beta_{35}$ , (c)  $\beta_{15}$ . Panels (a) and (b) show identified links within the confidence level and panel (c) shows a nonconnection. Panel (d) shows a difficult case from the larger network with 12 active electrodes. Initially the connection  $\beta_{53}$  is not significant, but as the filter gains more information about the network it becomes an identified link.

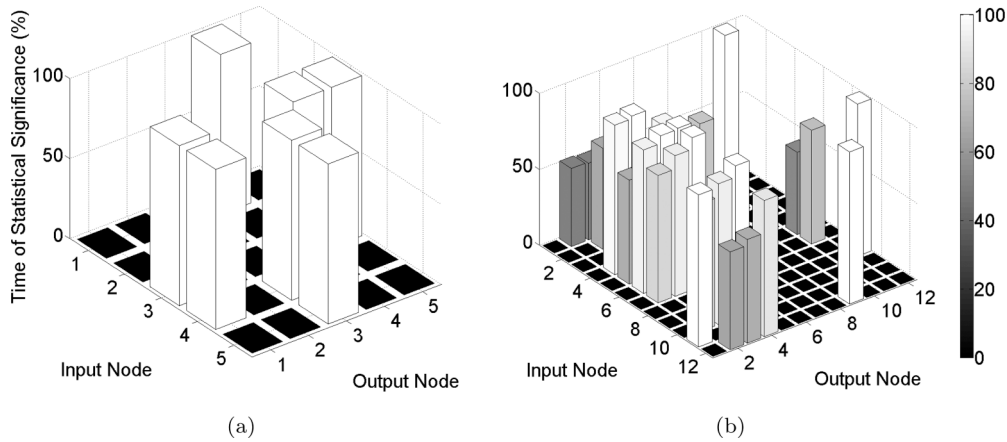


FIG. 5. Estimated network connection matrices for 160 sec of data from two MEA networks. The percentage time of statistical significance for (a) smaller network with five active electrodes and (b) larger network with 12 active electrodes is shown. A  $\beta_{ij}$  connection was determined to be significant by our method when its 95% confidence region did not include 0. In (a), 7 of 20 possible connections were found to be significant throughout the entire data set. In (b), 28 of 132 possible connections were found to be significant for at least 50% of the time interval.

that the connection exists, at least within the confidence level used.

Figure 5(a) shows the estimated network connection matrix and corresponding time of statistical significance for 160 sec of data from the small MEA network with five active electrodes at the 95% confidence level. Of the 20 possible connections in this network, only seven were determined to be statistically significant. These were found significant throughout the entire data series showing that our method was highly confident in their existence.

Figure 5(b) shows the estimated connection matrix computed from a 160-sec interval of data from the larger network with 12 active electrodes at the 95% confidence level. Out of the possible 132 connections, 28 were found to be significant at some time during the interval. This larger network presented questionable cases, typically whereby a connection parameter was initially not significant but became an identified link as more data were assimilated. All of the 28 connections that were statistically significant for part of the interval were significant for at least 50% of the interval, and 14 of the 28 were significant during more than 90% of the interval, as shown in the figure.

**V. CONCLUSION**

A method that can carry out sequential tracking of neuronal network links has a major advantage for experimental purposes. Using an EnKF with a general neuron model is a way to provide a statistically driven estimate of network connectivity that is updated continuously as data arrive, unlike offline methods such as [14–16]. This allows application to network structures with moderate nonstationarity, a typical feature of neural ensembles and biological networks in general. As shown above, this algorithm for detecting connectivity meets our criteria of being statistically based, robust to error, and capable of real-time implementation.

We showed in simulation and with measured data from neural cultures that such a method can work successfully. The choice of the model in the EnKF plays a critical role. Figures 2 and 3 illustrate the dependence on model mismatch. Certainly,

if the model is not representative of the basic dynamics of the underlying system, results will be compromised. A feature of this approach is that allowing parameters of the mathematical model in the EnKF to float may temper the mismatch between the dynamics of the model and the experimental system, resulting in more accuracy in the fitted connection parameters. A deeper study of the dependence on models is a fruitful direction for future work.

A related question is whether nonstationarity of the underlying system can confound attempts to find the correct connections. Undoubtedly this is true in some circumstances; in particular, the connections may be changing during the experiment. We attempt to minimize false conclusions by allowing parameters in the model to drift along with the data, to possibly correct for some of the nonstationarity in the experimental system, independent of the connections, but careful analysis of this possibility is beyond the scope of this work.

While the MEAs are plated at a high density of neuronal cells, observation of the network is restricted to the array’s 64 electrodes. While this may seem an undersampling of the network, tracking the connections between observed neural ensembles at each electrode may allow us to implement significant network control. This technique opens up several possible experimental strategies, including pharmacological and electrophysiological studies where the effects of an applied drug or pulse pattern on connectivity are to be determined. The ability to continuously track connectivity is designed to provide real-time feedback in an experimental situation, allowing an researcher to adjust observation, control, or other interventions.

Although we expect the statistical method outlined here to greatly expedite several proximate research goals such as tracking and control of neural cultures, the further objective of generalizing the application of this statistical method from cultures to the *in vivo* brain presents clear challenges. While the cultures present dynamics that are on the whole relatively nonsynchronous, activity arising from giant depolarizing potentials [30] and sharp wave ripple events [31] show

significant synchronicity, even in heterogeneous populations of cells. Extreme activity of this type could make network connectivity an unobservable quantity, due to the swamping of evidence necessary to determine cause and effect. In such cases, the method outlined here could be prevented from providing a reliable estimate of the link structure as long as the synchronization persisted. Further development of the method described here or complementary approaches for determining connectivity in these and other complex biological events is the subject of future work. Though these limitations

exist, implementation of our method in *in vivo* experimental situations such as those described in [32] and [33] could provide valuable insight to researchers.

#### ACKNOWLEDGMENTS

The research was partially supported by NSF Grants No. CMMI-1300007 and No. DMS-1216568. The manuscript was significantly improved due to the helpful comments of two reviewers.

- 
- [1] R. Dahlhaus, M. Eichler, and J. Sandkühler, *J. Neurosci. Methods* **77**, 93 (1997).
- [2] M. G. Rosenblum and A. S. Pikovsky, *Phys. Rev. E* **64**, 045202 (2001).
- [3] D. Napolitano and T. D. Sauer, *Phys. Rev. E* **77**, 026103 (2008).
- [4] C. W. J. Granger, *Econometrica* **37**, 424 (1969).
- [5] L. Sommerlade, M. Thiel, B. Platt, A. Plano, G. Riedel, C. Grebogi, J. Timmer, and B. Schelter, *J. Neurosci. Methods* **203**, 173 (2012).
- [6] D. R. Brillinger, *Ann. Probab.* **3**, 909 (1975).
- [7] A. Aertsen and G. Gerstein, *Brain Res.* **340**, 341 (1985).
- [8] A. M. Aertsen, G. L. Gerstein, M. K. Habib, and G. Palm, *J. Neurophysiol.* **61**, 900 (1989).
- [9] M. Garofalo, T. Nieuw, P. Massobrio, and S. Martinoia, *PLoS ONE* **4**, e6482 (2009).
- [10] E. S. Chornoboy, L. P. Schramm, and A. F. Karr, *Biol. Cybern.* **59**, 265 (1988).
- [11] M. Okatan, M. A. Wilson, and E. N. Brown, *Neural Comput.* **17**, 1927 (2005).
- [12] I. H. Stevenson, J. M. Rebesco, L. E. Miller, and K. P. Körding, *Curr. Opin. Neurobiol.* **18**, 1 (2008).
- [13] I. H. Stevenson, J. M. Rebesco, N. G. Hatsopoulos, Z. Haga, L. E. Miller, and K. P. Körding, *IEEE Trans. Neural Syst. Rehab. Eng.* **17**, 203 (2009).
- [14] G. N. Borisyuk, R. M. Borisyuk, A. B. Kirillov, E. I. Kovalenko, and V. I. Kryukov, *Biol. Cybern.* **52**, 301 (1985).
- [15] M. S. Masud and R. Borisyuk, *J. Neurosci. Methods* **196**, 201 (2011).
- [16] T. Berry, F. Hamilton, N. Peixoto, and T. Sauer, *J. Neurosci. Methods* **209**, 388 (2012).
- [17] R. Kalman, *J. Basic Eng.* **82**, 35 (1960).
- [18] E. Kalnay, *Atmospheric Modeling, Data Assimilation, and Predictability* (Cambridge University Press, Cambridge, England, 2003).
- [19] D. Simon, *Optimal State Estimation: Kalman,  $H_\infty$ , and Nonlinear Approaches* (John Wiley and Sons, New York, 2006).
- [20] J. Hindmarsh and R. Rose, *Proc. R. Soc. London, Ser. B* **221**, 87 (1984).
- [21] I. Belykh, E. de Lange, and M. Hasler, *Phys. Rev. Lett.* **94**, 188101 (2005).
- [22] H. Voss, J. Timmer, and J. Kurths, *Int. J. Bifurcation Chaos* **14**, 1905 (2004).
- [23] C. Trudinger, M. Raupach, P. Rayner, and I. Enting, *Environmetrics* **19**, 849 (2008).
- [24] G. Ullah and S. J. Schiff, *Phys. Rev. E* **79**, 040901 (2009).
- [25] G. Ullah and S. Schiff, *PLoS Comput. Biol.* **6**, e1000776 (2010).
- [26] D. Johnston and S. Miao-Sin Wu, *Foundations of Cellular Neurophysiology* (Bradford Books, Cambridge, MA, 1995).
- [27] A. Hodgkin and A. Huxley, *J. Physiol.* **117**, 500 (1952).
- [28] H. Hasegawa, *Phys. Rev. E* **61**, 718 (2000).
- [29] T. Berry and T. Sauer, *Tellus A* **65**, 20331 (2013).
- [30] S. Sipila, K. Huttu, I. Soltesz, J. Voipio, and K. Kaila, *J. Neurosci.* **25**, 5280 (2005).
- [31] W. Ramadan, O. Eschenko, and S. Sara, *PLoS ONE* **4**, e6697 (2009).
- [32] G. Buzsaki, *Nat. Neurosci.* **7**, 446 (2004).
- [33] M. Nicolelis, D. Dimitrov, J. Carmena, R. Crist, G. Lehw, J. Kralik, and S. Wise, *Proc. Natl. Acad. Sci. U.S.A.* **100**, 11041 (2003).